Analysis on Device Mechanism and Numerical Simulation of Composite Air Purification

Jianlong Liu[1, 2*], Peng Liu[1], Li Liu[1] and Haiping Zhang[1]

*[1]College of Civil Engineering, Hunan University of Technology, Zhuzhou, 412007, China;
[2]Collaborative Innovation Center of Building Energy Conservation & Environmental Control, Zhuzhou, 412007, China;
ljlphd@sina.com

Abstract

To solve the technical problems existing in air purification, a multileveled air purification device is presented. And the new device consists of catalytic purifying technology, low-temperature plasma, nanoscaled titania and dual-band ultraviolet. To deeply take a research on performance of the composite purification device, the device has been numerically simulated, with CFD simulation technology, through employing gas phase turbulence model, porous medium model and stochastic particle trajectory model. Comparative analyses on pressure distribution of internal flow field, velocity distribution, particle motion state and mass concentration distribution are made under different wind speed. The most appropriate wind speed can provide better centrifugal effect and less pressure loss. So some rules of velocity, pressure distribution and the particulate mass concentration distribution at all levels after filtering in internal device are acquired. In the meanwhile, a comparison among different research results has been made, and it helps to prove the reliability of this method.

Keywords: Composite air purification device; Velocity field; Pressure drop; Numerical simulation

Introductions

Welding was an indispensable technical means in industry. It has played an important role in development of the national economy. However, smoke and dust produced by bonding technology caused serious environmental pollution and endangered the people's health. Control of welding fume was always a big problem in the field of industrial ventilation, and the difficulty mainly existed in the large-scale trend of welding workshop, uncertainty of welding location, diversity of welding modes and the complex diffusion mechanism of welding fume [1]. Volatile organic pollutant emissions in the welding workshop (VOCs), inorganic pollutants like SO_2, NO_x, and welding fume have threatened both human health and environment. A huge development of technologies in treating welding fume has been seen since people paid more attention to treatment of welding fume with a stricter standard on industrial environment in recent years in China. The traditional air purification technology, such as heat / catalytic combustion method, biological filtration, membrane separation and selective reduction technology had such disadvantages as large investment, long cycle and high operation cost.

Thus, it is necessary to find out new methods and ways to efficient composite air purification [2]. Domestic and foreign experts also made several profound researches in this area. The plasma welding fume purification device was invented by Gang Chen and Bo Zhang [3], improving the efficiency of purification through optimization design of plasma producing ring and HVDC pulse power. The experiments showed that the

purification efficiency, compared with traditional devise, had been improved by 70 to 80 percents. The plasma/photocatalysis coupling air purification device invented by Lian Hou and Zuguo Wu[4] was a gaseous pollutant purification device that based on plasma and photocatalysis coupling technologies, and researches proved that the purification efficiency could reaches 80% in treating special gaseous organics within one hour, the dust removal rate achieve 96.9%, the bactericidal rate 100%, the maximum air outlet 538.4m³/h and the noise in normal rating 55dB. To solve technical problems existing in air purification, a multilevel air purification device was presented [5]. And the new device is a combination of catalytic purifying technology of low-temperature plasma, nanoscaled titania and dual-band ultraviolet.

To take further a research on mechanism of the composite air purification, simulation technique of computational fluid dynamics is adopted by using the software Fluent[6] to create the physical model of the composite air purification, simulating welding fume flow inside the device and verifying the feasibility of composite air purification device. Finally, all of these can provide a theoretical basis for the design and optimization of the new device.

1. Structure and Principles

1.1. Structure of Composite Purifying Device

The composite air purification device [7-8] is a multileveled purifying method which consists of technologies of low-temperature plasma, nanoscaled titania and dual-band ultraviolet. The new device can improve cleaning efficiency. At the same time, it also has the ability to adsorb and regenerate activated carbon. Thus, it can not only improve the removal efficiency of harmful gas, but also prolong the service life of activated carbon. The composite air purification device consists mainly of three parts---a primary filter, a catalytic filter of low-temperature plasma, nanoscaled titania and dual-band ultraviolet, and a high efficiency air filter (Figure 1).
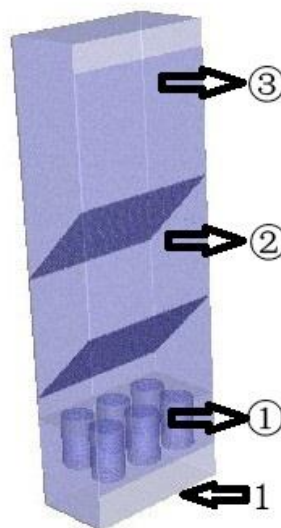

Figure 1. Composite Purifying Device Structure Diagram

1.2. The Purification Mechanism Analyses

The purification efficiency of this device refers a ratio of the concentration difference, which is between the inputted & outputted pollution and the inputted pollution concentration. The purification mechanism of this equipment: impacted by negative pressure generated in the centrifugal fan, welding fumes enter the purification device through inlet one, and start the first filtration when it passes the primary filter（①）, larger and heavier particles will, in the process of initial impaction with filter, change their motion direction and subsequently be captured when directly hitting the filter screen, particles above 5μm and suspended matters are mainly treated in this level, and it also can filter some PM10(inhalable particles) and most welding fume, the purification efficiency is about 90%(mainly focusing on purification of solid particles), the harmful gases subsequently step into the secondary filtration （②） after passing the first filter. It first ionizes and oxidizes such matters as bacteria, virus and TVOC, when and after the high frequency plus discharging, basic gases get a sufficient amount of energy; then it absorbs radiation from ultraviolet in photocatalyst and is activated to generate free ions, electronics and holes. Therefore, it can decompose such harmful substances as carbon monoxide, titrogen oxides, hydrocarbons, aldehydes and benzene, all of which will be catalyzed and reduced to environment friendly and pollution-free chemicals, such as H_2O and CO_2; the filtering efficiency in this process is 82.4%(mainly focusing on purification of pollution). Finally it steps into the third filtration process （③）, in this level, the main task is to exclude dust microorganisms and suspended matter, as well as further purifying the byproducts generated in treatment in previous purification processes; in this process, the filtering efficiency is approximately 99.99%(mainly focusing on solid particles and microorganisms above 0.3μm). The entire purification efficiency of this air purification device in treating air pollution can reach 85% and even more, which is higher by 5% ~ 10% than the same kinds of devices.

2. Numerical Simulation Calculations and Results Analyses

The rotational speed of centrifugal fan affects flow velocity of gas. The welding fume may pass through the filter without full inertia separation if the rotation speed reaches too high. On the contrary, there might be not enough centrifugal force produced if the speed is too slow. When the cross sectional area is fixed, ventilation volume is proportional to velocity; On the other hand, when the ventilation rate increases, pressure loss of the device will increase. In order to acquire highly efficient energy of purification device, appropriate speed should be selected, and it can help to acquire a higher ventilation volume and also can keep a lower amount of pressure loss. Through adopting computational simulation technology of fluid dynamics and gradually increasing centrifugal fan speed, the situation is simulated when welding fumes passing through purification device, the flow velocity of welding fumes, pressure changed and trajectory of particles could be observed. In this way the optimum speed could be found. The air volume and pressure loss in the device achieves the optimal allocation.

3. Computational Modeling and Grid Division

3.1. The Gas Phase Turbulence Model

It is the RSM model that can well predict fan's strong turbulence field in the composite device. Transport equation of the stress of each component is shown in formula (1):

$$\frac{\partial}{\partial t}\left(\rho \overline{u_i u_j}\right) + \frac{\partial}{\partial x_k}\left(\rho U_k \overline{u_i u_j}\right) = D_{ij} + P_{ij} + \prod_{ij} \cdot \varepsilon_{ij} \tag{1}$$

In the formula: $\frac{\partial}{\partial t}\left(\rho \overline{u_i u_j}\right)$ is the time rate of change of stress(transient term), $\frac{\partial}{\partial x_k}\left(\rho U_k \overline{u_i u_j}\right)$ is a convection term, D_{ij} is the term of stress diffusion, $D_{ij} = \frac{\partial}{\partial x_k}\left[\frac{u_i}{\delta_k}\frac{\partial \overline{u_i u_j}}{\partial x_k}\right]$, turbulent viscosity in this equation is determined by $u_i = \rho C_u \frac{k^2}{\varepsilon}$, P_{ij} is the shear generated term, and there is no simulation for P_{ij}, $\prod_{ij} \cdot \varepsilon_{ij}$ is a term of pressure-strain and pressure dissipation; $\varepsilon_{ij} = \frac{2}{3}\delta_j\left(\rho\varepsilon + Y_M\right)$, in the equation, $Y_M = \rho\varepsilon 2M_t^2$, M_t refers mach number, scalar dissipation rate ε can be calculated by equation of dissipation rate transport in $k-\varepsilon$ model. When the composite air purifying device simulates fan's gas flow field, the pressure strain term $\prod_{ij}$ should be improved [9], and it can be calculated by difference scheme QUICK and be determined by algorithm SMPLEC.

3.2. Porous Media/Fluid Coupling

Based on the models of porous media, the unsteady axisymmetric correction N-S equation is drawn for compressible fluid by N-S equation

$$\frac{\partial'}{\partial't}\iiint_V a_V Q dV + \iint_s a_n n \square A dS = \iiint_V a_V \frac{S}{r} dV + \iiint_V a_V \frac{S_{por}}{r} dV$$

In the equation, av is volumetric porosity, an is the surface penetration rate for n direction of outward normals of integration surface, defying the ratio of porous area and the entire area, $A = (E - E_v)e_x + (F - F_V)e_r$, E and F are viscous flux for both x and r direction, S is the source item for symmetric N-S equation and Spor is the resistance and item results from heat source.

3.3. Geometry Modeling and Grid Division

Geometric model of composite air purification device is generated [10] by software GAMBIT, and in this device geometric parameters of concrete are as follows: The box is 1240mm in length, 640mm width, 3640mm height, import and export area is 1240mm × 200mm.

We use finite volume method for grid generation. The composite air purification device contains a cylindrical primary filter, whose structure is complex and asymmetrical. Compared with structured grid, unstructured grid computing process is more complex, however, its local refinement is relatively easy. It can adapt to irregular graphics without many difficulties and show the fine structure of flow field. Tetrahedral unstructured grid is chosen to divide the primary filter and the imports & exports. Some important region is of unstructured local refinement. The cuboid is divided by using tetrahedral structured grids, generating about 2070000 grids (Figure 2).
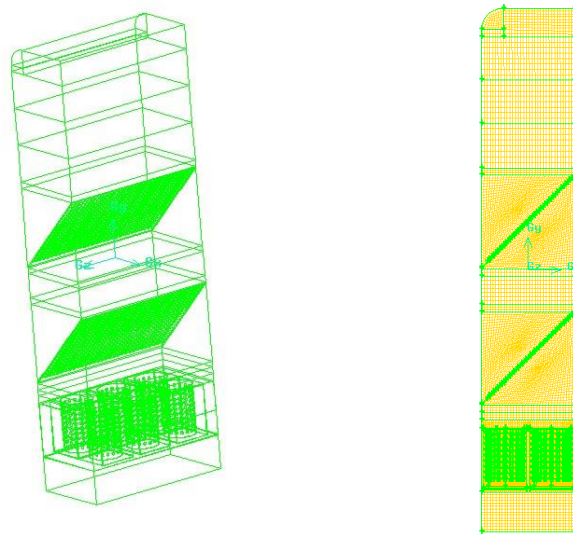
Figure 2. Geometry Modeling and Grid Division

3.4. The Boundary Condition Set

3.4.1. Entrance Boundary Condition

Velocity boundary is selected as the entrance boundary condition. Velocity of gas phase and particle phase in entrance is respectively set as follows, v=3m/s, v=4m/s, v=5m/s. Density of particles phase is 3000kg/m3.

3.4.2. Outlet Boundary Condition

The escape boundary condition is set as the outlet boundary, and the particle phase is set as the complete escape.

3.4.3. Boundary Condition of Particle Phase

It is hypothesized that the particles in the purifying device have good following behaviors. So there is no relative slip velocity, and initial velocity, which is uniformly distributed at the entrance, is consistent with the continuous phase.

3.4.4. Porous Media

The porous media take solid media as a skeleton, containing a lot of capillary pore space, some of which are highly linked with each other. Fluid is media which can both reserve and flow in these spaces. Because the effective filter net is a porous screen structure, which is included in porous media, porous jump is chosen to lead the calculation.

3.5. The Grid Independence and Confirmation of Simulation Results

Figure 3 shows simulation results comparison of particles mass concentration in different grid numbers. When grid number is more than 1900000, the calculations are similar; therefore, the grid number is set as 2,070,000.
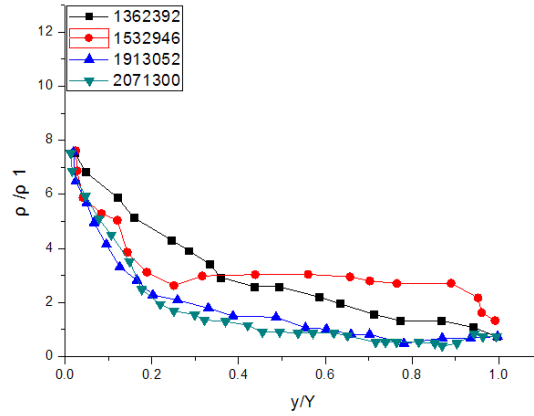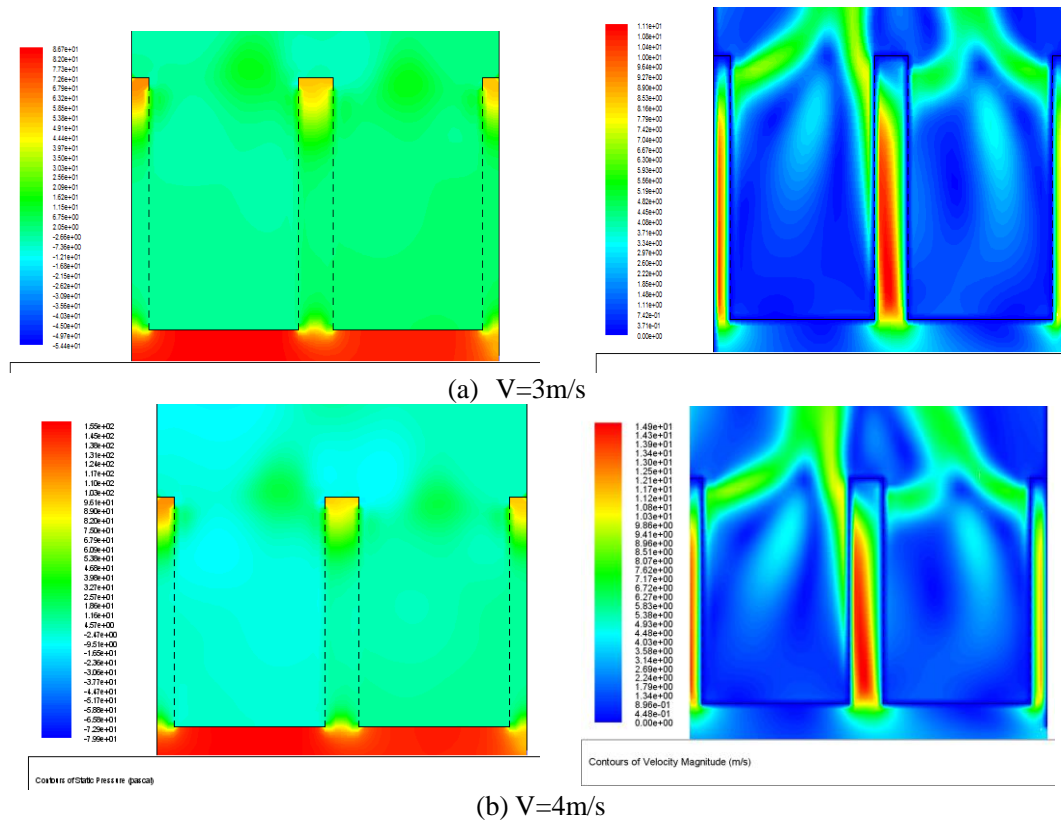
Figure 3. Mass Concentration Distributions of Particles in Different Grid Numbers

4. Results and Analyses

4.1. Pressure & Velocity Distribution of Primary Filter in Composite Air Purification Device
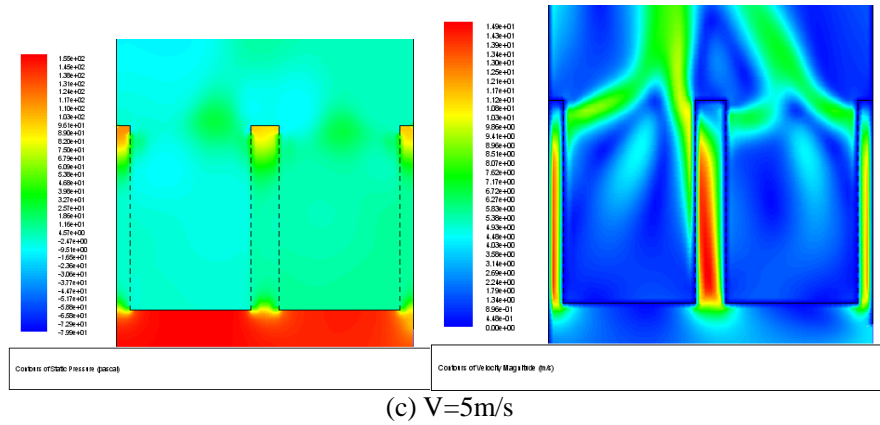

(a) V=3m/s

(b) V=4m/s

(c) V=5m/s

Figure 4. Pressure & Velocity Distribution in the Primary Filtering Cartridge

Figure 4 shows pressure and velocity distribution in the primary filter when Z=0mm. As shown in the figure, regional pressure in filtering cartridge is generally negative, which is caused by the expended zone of negative pressure in the composite air purification device when rotation speed of the fan on the upper side increases; strong wind at filtering cartridge entrance is caused by increased pressure difference in filtering cylinder on either side. As the speed increases, the negative pressure region gradually increases. It shows that velocity increases with the bigger pressure, which may also cause a more obvious direction change of air flow when it passing through the filtering cartridge, and finally lead to a better filtering effect of the filtering cylinder.

4.2. Pressure and Velocity Distribution of Needle Plate-Type Low-Temperature Plasma Generator in Composite Purification Device

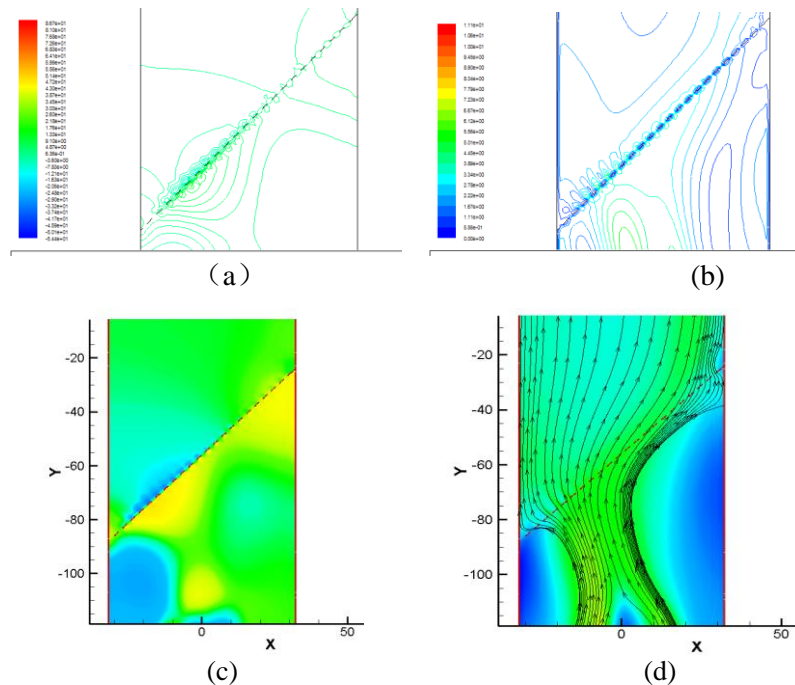（a）　　　　　　　　　　　　　　（b）

(c)　　　　　　　　　　　　　　(d)

Figure 5. Pressure and Velocity Distribution Of Needle Plate-Type Low-Temperature Plasma Generator

a & b respectively for the pressure and velocity distributions;
C & d respectively for pressure nephogram and velocity streamline nephogram

Figure 5 shows the distribution of pressure and speed when Z=0mm. As we can see, when entering the device, airflow is relatively concentrated, and it starts to separate after passing the needle-plate low-temperature plasma generator. Compared with primary filter's pressure, the pressure is smaller as it is closer to the outlet, and the pressure gets bigger in negative pressure region at the outlet boundary when the fan speed gradually increases. As shown in Figure 5, the greater the rotation speed is, the bigger the flow velocity at the edge of needle-plate low-temperature plasma generator, and the more obvious effect on the airflow distribution. However, larger pressure differences in front of and behind of the needle-plate generator will be accompanied by a greater rotation speed. It indicates that air flow will rotate when the centrifugal force reaches too high, but it also produces greater resistance. Therefore, appropriate rotation speed should be the one that can form a strong centrifugal force with less pressure loss.
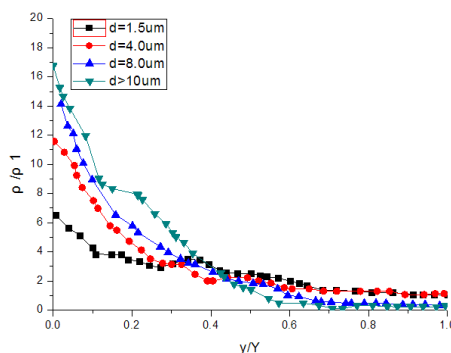
4.3. Particle Mass Concentration Distribution

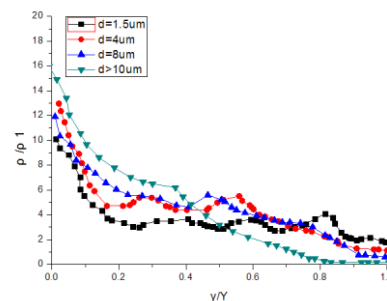**Figure 6. Particle Mass Concentration Distribution at Section X=200mm**

Figure 7. Particle Mass Concentration Distribution at Section X=0mm

Figure 6 shows particle mass concentration distribution when space section x=200mm. For 1.5um particles, mass concentration shows a decreased distribution. In the range of y/Y=0~0/35, with increased particle size, particle mass concentration increases along the Y axis and the concentration also increases with the larger particle size. It shows that in the initial stage, there are more large particles in the air. For distribution of different particle size, the mass concentration decreases when the value of y/Y increases, and it reveals that the particles have been removed level by level when they are passing every purification stage, and eventually it reaches the mass concentration rage which is harmless to health. Figure 7 shows particle mass concentration distribution when space section x=0mm. Compared to Figure 5, for 1.5μm particles, mass concentration tends to be a wave dynamic distribution, which can be divided into center carry zone, low mass concentration zone and high mass concentration zone near the wall. As the particle size increases, the low mass concentration region slightly expands, increasing the mass concentration near the wall in the high mass concentration zone. Along the Y axis, particle mass concentration shows a decreasing trend, which indicates that particles are filtered through multistage filter and that composite air purification device has a good performance.

As calculated and analyzed above, it can be set that the mass concentration of large particles is high when it is in the entrance, and it indicates that the particles have been removed level by level when they are passing every purification stage. After a analysis on fluid field at the wind speed of 3m/s, 4m/s and 5m/s, we find that the devise can not only keep a good filtration effect but also will not generate too much pressure loss even when the velocity reaches too high when the speed is constant at 4m/s.

4.4. Numerical Calculations and Results Comparisons

To verify the flow field function and the distribution of mass concentration of particles of the multileveled air purification device, the sample of this purification is invented, changing the input wind speed to 3m/s, 4 m/s and 5 m/ and employing the Tude400 multifunctional measuring device to measure the flow field. Which had been recorded, inside of the purification device, as is shown in Figure 8, under different wind speed, the tested rule of distribution of internal flow speed in the purification device is slightly smaller than the numerical calculated results. However, the two results of internal fluid field of purification device tend to be the same under a different wind speed. Using No. 3330 optical particle size device to measure the mass concentration of particles, and comparing the tested results (Figure 9) with numerical calculated results(Figure 6), it is found that the tested rule of particles' mass distribution inside of the purification device is larger than the numerical calculated results, which shows the difference between tested results and theoretical results. However, the rule of mass concentration of particles in purification device is the same for both numerical calculated and tested results, which further verifies the accuracy of the experiment.
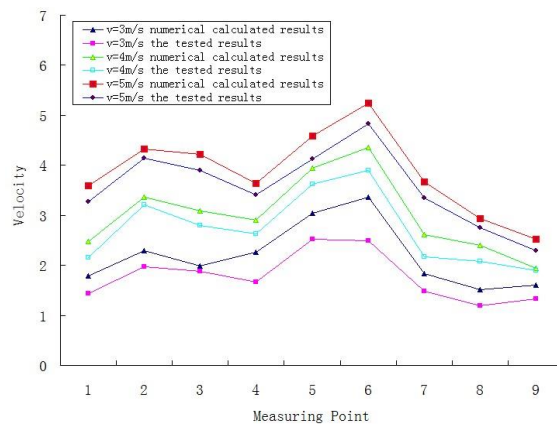

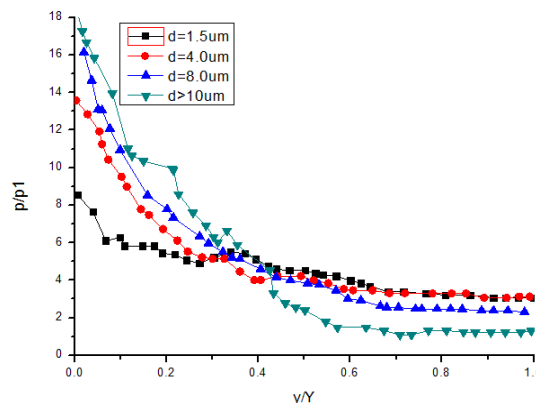**Figure 8. Tested Results of Speed Distribution at Each Measuring Point**

Figure 9. Tested Results of Distribution of Mass Concentration

5. Conclusions

(1) The composite air purification device can use the primary filtering barrel to easily remove larger or heavier particles. It can purify dust and particles well since they will change direction and subsequently hit the filter screen and be captured when they are in the initial impaction with the first filter, the efficiency in purifying harmful particles in the air reaches 90%.

(2) We lead a 3D numerical simulation of internal flow filed for inner space of the composite air purification device, especially focusing on the primary filtration process and needle-plate low-temperature plasma region. Comparisons and analyses are made for difference wind velocity, distribution of pressure and velocity as well as the motion state of particles with same diameter on y axis section both in primary filtration and needle-plate low-temperature plasma region. According to the analysis results, the greater wind speed, the greater centrifugal force particles may get, and the better purification effect on soot particles. At the same time, pressure difference before & after the filter has also increased sharply, which increases pressure loss of the purification device.

(3) The distribution of compressible fluid is described in the area of porous media/fluid coupling through the idea of using the model of porous media and correction N-S equation and employing CFD technology to solve the equation .The advantage of this way is that the matching condition in the interface can automatically meet, which reduces the complexity of calculation.

(4) Through testing the sample device, as shown in this figure that the tested results and numerical results are the same, which verifies the accuracy of the experiment. Moreover, setting gas phase turbulence model, porous media model and particle randomly tracking model can provide an excellent simulation for multilevel air purification device.

Acknowledgements

Reference

[1] X.-X. Ma, C. Li and H. Liu, "Test on effects of displacement ventilation in welding plant with adequate space", Journal of Electric Welding Machine, (**2011**), vol. 41, no. 2, pp. 48-51.

[2] J. Liu, Y. Chu and H. Wang, "Numerical simulation and analysis of NTP and catalytic reactor", Applied Mechanics and Materials, vol. 353-356, (**2013**), pp. 3683-3690.

[3] G. Chen, B. Zhang and J. Chun, "The Development of Carrying Charge Device for Purifying Soot of Weld by Plasma", High Voltage Engineering, (**2002**), vol. 28, no. 8, pp. 29-30.

[4] L. Hou, Z. Wu and Y. Wang, "Develop a Equipment for Air Purification by High Voltage Pulse Plasma", Development & Innovation of Machinery & Electrical Products, vol. 22, no. 4, (**2009**), pp. 17-18.

[5] Y. Lu, C. Ma and W. Wang, "Research on photocatalytic technology of sterilization and air purification", Journal of Engineering Thermophysics, vol. 25, no. 2, (**2004**), pp. 311-313

[6] Z. Han, X. Shao and Z. Ou, "Design method of combined air cleaners in urban underground spaces", Journal of Heating Ventilating and Airconditioning, vol. 40, no. 12, (**2010**), pp. 1-8

[7] T. Xu, G. Chen and R. Niu, "Study on Air Purification by Plasma Combined With Photocatalysis", Journal of Environment and Health, (**2006**), vol. 23, no.6, pp. 535-536.

[8] P. Li, M. Xu and F. Wang, "Proficient in CFD engineering simulation and case of actual combat", Beijing: Posts & telecom press, (**2011**).

[9] M. Ghiaci, A. Abbaspur and M. Arshadi, "Internal versus external surface active sites in ZSM-5 zeolite Part 2: Toluene alkylation with methanol and 2-propanol catalyzed by modified and unmodified H3PO4/ZSM- 5", Applied Catalysis A: General, (**2007**), vol. 316, no. 1, pp. 32246.

[10] W. Nie, W. Cheng and Y. Yao, "Numerical Simulation of Vortex Air Curtain Suction Dust Control System and Its Applications", Science ＆ Technology Review, (**2011**), vol. 29, no. 9, pp. 48-52.

Authors

Liu Jianlong (1974-) , male, Yiyang City, Hunan Province, Doctor, Associate Professor;

Research field: Building environment and indoor air quality. In recent years, more than 100 papers published in domestic and foreign well-known publications and international conferences.